JPET Fast Forward. Published on November 5, 2018 as DOI: 10.1124/jpet.118.250225
This article has not been copyedited and formatted. The final version may differ from this version.

Suppression of canine ABCB1 in MDCKII cells unmasks human ABCG2-mediated efflux of olaparib

Yoo-Kyung Song, Ji Eun Park, Yunseok Oh, Sungwoo Hyung, Yoo-Seong Jeong, Min-Soo Kim, Wooin Lee and Suk-Jae Chung

College of Pharmacy, Seoul National University, 1 Gwanak-ro, Gwanak-gu, Seoul, 08826, Republic of Korea (Y.-K. S., J. E. P., Y. O., S. H., Y.-S. J., M.-S. K., W. L., S.-J. C.)

Running title: hABCG2-mediated efflux of olaparib in cABCB1-suppressed MDCK

Correspondence to: Suk-Jae Chung, Ph.D.

College of Pharmacy

Seoul National University, 1 Gwanak-ro, Gwanak-gu, Seoul, 08826, Republic of Korea

Telephone: +82-2-880-9176; Fax: +82-2-885-8317; E-mail: sukjae@snu.ac.kr

Document Statistics:

Text pages: 43

Tables: 2

Figures: 5

References: 44

Abstract: 221

Introduction: 561

Discussion: 1180

Abbreviations:

cER, corrected efflux ratio; cABCB1, canine ABCB1 transporter; ER, efflux ratio; hABCG2, human ABCG2 transporter; MDCKII, Madin-Darby canine kidney cell type II; P_{app}, apparent permeability coefficient; qPCR, quantitative real-time polymerase chain reaction; shRNA, short-hairpin RNA.

Recommended section assignment:

Metabolism, Transport, and Pharmacogenomics

Abstract

Endogenous cABCB1 is expressed abundantly in MDCKII cells, and its presence often complicates the phenotyping of the transport process. Errors in estimating cER, as the result of the variable expression of cABCB1, were examined for the dual substrates of ABCB1 and ABCG2 in MDCKII cells expressing hABCG2. The mRNA and protein expression of cABCB1 was 60% and 55% lower, respectively, in MDCKII cells expressing hABCG2 compared to the values for the wild type, suggesting that the expression of endogenous cABCB1 became variable after the expression of hABCG2. To minimize the contribution of endogenous efflux, cABCB1 was suppressed kinetically (i.e., using verapamil as a selective inhibitor), or biochemically (i.e., transfecting short-hairpin RNA against cABCB1). Under these conditions of suppression, the cER values for irinotecan and topotecan, dual substrates of ABCB1 and ABCG2, were elevated by over 4-fold and 2-fold, respectively, in comparison to the values without the suppression. The cER of olaparib was similarly increased to 3- and 5-fold in MDCKII cells under the kinetic and biochemical suppression of cABCB1, respectively, suggesting that hABCG2-mediated efflux cannot be ruled out for olaparib. Since the substrate selectivity for ABCB1 and ABCG2 is considerably overlapped, the possibility of an inaccurate estimation of cER needs to be taken into consideration for the dual substrates in the case of the variable expression of cABCB1 in MDCKII cells.

Introduction

MDCKII cells are frequently used in bi-directional transport assays in studies of the functional involvement of efflux transporters (Tang et al., 2002). The reasons for the widespread use of this cell line may include a relatively rapid development in the tight junction, easy maintenance and the fact that MDCKII cells expressing foreign transporters are readily available. In fact, some regulatory agencies (e.g., FDA) recently recommended the use of MDCKII cells as one of the assay systems in phenotyping efflux transporters (e.g., ABCB1 and ABCG2) for substrates (FDA, 2017). Despite their utility, however, wild type MDCKII cells express a relatively abundant number of canine transporters (e.g., cABCB1) (Goh et al., 2002), thereby complicating the phenotyping of the transport process(es). The method of 'corrected' efflux ratio (cER), the ratio of the ER calculated in cells expressing a foreign transporter to that in control cells, is frequently used to account for the contribution of endogenous transporters. In general, a cER value greater than 2 is regarded as a reasonable threshold (FDA, 2017) for the indication of a contribution of an efflux transporter. This type of correction, however, would only be valid when the baseline function of endogenous transporters remains constant within the study period. In practice, however, the importance of demonstrating the stationary function of an endogenous transporter appears to be less well appreciated: For example, validation of the consistent function of endogenous transporters in cell lines is not mandatory in the guidelines from the regulatory agencies. In contrast, there is ample evidence in the literature wherein routine maintenance can lead to the variable expression of endogenous transporter(s) (Xia et al., 2005; Siissalo et al., 2007). In a recently reported study, Kuteykin-Teplyakov and co-workers (Kuteykin-Teplyakov et al., 2010) showed that the functional expression of a foreign transporter led to variations in the expression of endogenous transporter(s) and therefore to an inaccurate estimation of cER. It

is noteworthy that the authors found that the functional expression of cABCB1 was reduced in MDCKII cells expressing human ABCB1 (hABCB1), resulting in a cER value of less than 1.5 (viz, the value indicating an unlikely substrate) for vinblastine, one of the most well characterized substrates of hABCB1 (Kuteykin-Teplyakov et al., 2010; Li et al., 2013). These observations suggest that the cER method, as it is currently used, is not reliable for the phenotyping of transport process in MDCKII cells when endogenous transporter(s) are not expressed at constant levels.

In our routine transporter phenotyping study, we found that the basolateral to apical transport of olaparib, a known hABCB1 substrate, was strongly inhibited in MDCKII cells expressing hABCG2 in the presence of Ko143, a standard hABCG2 inhibitor (Allen et al., 2002), at concentrations that would be ineffective in suppressing cABCB1 function, implying that the anticancer agent may be an hABCG2 substrate. However, this implication is in direct contradiction to the conclusions reported in a European Medicines Agency's assessment report for olaparib (CHMP, 2014). In theory, such an inconsistency may be a manifestation of the inadequate estimation of cER due to the variable function of an endogenous transporter(s) such as cABCB1, although this possibility was not directly examined in the study cited. The objectives of this study, therefore, were to determine the possibility that endogenous cABCB1 is expressed at variable levels in MDCKII cells expressing hABCG2, and its impact on estimating the cER of olaparib, a potential substrate for both ABCB1/ABCG2.

Materials and Methods

Chemicals and reagents

[^{3}H]-Digoxin (specific activity 39.8 Ci/mmol) and [^{3}H]-prazosin (specific activity 84.2 Ci/mmol) were purchased from Perkin Elmer (Waltham, Massachusetts). Unlabeled digoxin, imipramine, Ko143 hydrate, verapamil, tariquidar, zosuquidar, and topotecan were obtained from Sigma-Aldrich (St Louis, MO, USA). Olaparib [the purity over 99%; LC laboratories (Woburn, MA, USA)] was also used in this study. Unlabeled prazosin and irinotecan were purchased from Tokyo Chemical Industry (Tokyo, Japan) and Cayman Chemical (Ann Arbor, MI), respectively. High-performance liquid chromatography-grade methanol and formic acid were purchased from Fisher Scientific (Pittsburgh, PA, USA) and Fluka (Cambridge, MA), respectively.

Cell lines and Cultures

Cells from a wild type MDCKII (MDCKII/WT) cell line (passage number from 47 to 60) (European Collection of Authenticated Cell Culture, Salsbury, UK) and LLC-PK1 cell line (passage number from 196 to 221) (American Type Culture Collection, Rockville, MD) were used in this study. MDCKII cells were grown in Dulbecco's modified Eagle's medium (Welgene Inc., Daegu, Korea) containing 10% fetal bovine serum (Welgene Inc., Daegu, Korea), 1% nonessential amino acid solution, 100 units/mL penicillin, and 0.1 mg/mL streptomycin under a humidified atmosphere of air containing 5% CO_2 at 37°C, and cultured under previously described conditions (Lee et al., 2015; Hyung et al., 2017; Yim et al., 2017).

Generation of MDCKII/hABCG2 and LLC-PK1/hABCG2 cells

In this study, a commercially available plasmid construct containing cDNA for hABCG2 (pCMV6-AC; Origene, USA) was transfected to functionally express the human transporter.

MDCKII wild type cells (MDCKII/WT, passage number of 49) and LLC-PK1 wild type cells (LLC-PK1/WT, passage number of 202) were seeded in 12-well plates 24 hours prior to transfection. When the cells reached a 50~70% confluence, they were transfected using the FuGENE® HD Transfection Reagent (Promega, Madison, WI) according to the manufacturer's instructions. Briefly, 2 μg of the plasmid DNA was transfected with 6 μL of the transfection reagent mixed with Opti-MEM (Thermo Fisher Scientific, USA), and the cells were transferred to a 100-mm dish after 24 hours of transfection. Geneticin was introduced to the media at a concentration of 0.6 mg/mL and 1 mg/mL (for MDCKII and LLC-PK1 cells, respectively) on the next day of the cell transfer. The selection media were maintained for at least 14 days to select the clones resistant to the antibiotics. A Hoechst®33342 dye efflux assay (Scharenberg et al., 2002) was then carried out to select the clone having the most distinct functional expression (i.e., the least fluorescent clone) of the transporter. When necessary, semi-quantitative PCR analysis was carried out using the following the primers and cycling conditions: 5'-GCCTCACCTTATTGGCCTCA-3' and 5'-AGTTCCACGGCTGAAACACT-3' for *canine ABCB1*; 5'-AGATTGTCAGCAATGCCTCC-3' and 5'-GAGCTTGACAAAGTGGTCATT-3' for *canine GAPDH*; 5'-GAGTGAACGGATTTGGCCGC-3' and 5'-TCTCATGGTTCACGCCCATC-3' for *porcine GAPDH*; PCR conditions consisted of denaturation in 94˚C for 30 sec, annealing at 56˚C for 30 sec and elongation in 72˚C for 2 min 30 sec. A bi-directional transport study of [^{3}H]-prazosin (i.e., primarily a substrate for hABCG2; along with unlabeled prazosin; final concentration of prazosin to be 1 μM) (Lepist et al., 2012; FDA, 2017) was carried out for further confirmation of the functional expression. In this study, the ER of prazosin at a value greater than 9 (i.e., for MDCKII/hABCG2; in comparison to the ER of 1 in MDCKII/WT) or 7 (i.e., for LLC-PK1/hABCG2; in comparison to the ER of 2.4 in LLC-PK1/WT) was accepted as an indication of the functional expression

of the efflux transporter (Fig. S1 and Fig. S2, Supplemental material) and was used in subsequent studies.

In parallel, mock-transfected MDCKII and LLC-PK1 cells were also generated by transfecting the wild type cells with the corresponding empty vector. For MDCKII cells, a bi-directional transport study of [^{3}H]-digoxin (i.e., primarily a substrate for cABCB1; along with unlabeled digoxin; final concentration of digoxin to be 1 μM) was carried out to compare the functional activity of cABCB1 in transfected and un-transfected cells. In our study, mock-transfected and wild type MDCKII cells showed a comparable functional expression of cABCB1 (i.e., ER of digoxin was 6.7 in MDCKII/Mock, compared to an ER of 6.3 in MDCKII/WT). Thus, in subsequent studies, MDCKII/WT cells were considered to be functionally identical to MDCKII/Mock cells and were used as controls in the estimation of cER.

Quantitative real-time PCR (qPCR)

To determine the extent of target mRNA in MDCKII cells, a qPCR study was carried out using standard protocols. Briefly, total RNA was extracted from MDCKII cells using the HybridR RNA extraction kit (GeneAll, Korea) and reverse-transcribed with an oligo dT primer using a PrimeScript RT-PCR kit (Takara, USA) according to the manufacturer's instructions. Amplification was detected by TOPreal ™ qPCR 2× PreMIX with SYBR Green (Enzynomics, Korea) on a StepOnePlus™ Real-Time PCR system (Applied Biosystems, USA). Thermocycling was carried out using a reaction mixture of 15 μL [i.e., 7.5 μL premix, 0.1 μL of forward and reverse primers (final concentration at 0.1 μM), 6.3 μL of PCR grade water, and 1 μL target cDNA]: The sequences for the forward and reverse primers were 5'-TTGCTGGTTTTGATGATGGA-3' and 5'-CTGGACCCTGAATCTTTTGG-3', respectively, for *cABCB1* (Kuteykin-Teplyakov et al., 2010) and 5'-

ATTCCACGGCACAGTCAAG-3' and 5'-TACTCAGCACCAGCATCACC-3', respectively, for c*GAPDH* (Kuteykin-Teplyakov et al., 2010; Gartzke et al., 2015). In this study, the reaction mixture that did not contain a template was considered to be a negative control in the study. The conditions for the thermal cycling consisted of an initial activation of DNA polymerase for 10 min at 95˚C, followed by 50 cycles of amplification at 95˚C for 10 s, 60˚C for 15 s and then 72˚C for 30 s with a final melting step of 95˚C for 15 s. In this study, the level of canine *GAPDH* mRNA detected in the amplification was used for normalization of the level of the target mRNA.

Western blot analysis

Western blotting analysis was carried using total cell lysates. Briefly, MDCKII cells were lysed with lysis buffer containing protease inhibitors (Complete®; Roche, IN, USA). After brief centrifugation (10,000 g, 10 min, 4°C), the resulting supernatant was analyzed by a bicinchoninic acid assay (Smith et al., 1985). Samples containing an equivalent amount of total protein (60 µg) were mixed with Laemmli buffer (Laemmli, 1970) and heated at 50°C for 30 min. The heated samples were resolved by 7.5% sodium dodecyl sulfate-polyacrylamide gel electrophoresis. Subsequently, the blot was prepared using a poly (vinylidene) fluoride membrane and incubated in a 0.05% Tween 20/phosphate buffered saline (TPBS) solution containing 3% bovine serum albumin (BSA) for 1 hour to block non-specific binding. For the detection of cABCB1, the membrane was probed using the commonly used anti-ABCB1 antibody C219 (Biolegend, USA; dilution 1:200, 3% BSA in TPBS) (Kuteykin-Teplyakov et al., 2010; Gartzke and Fricker, 2014; Gartzke et al., 2015). As a gel-loading control, the membrane was probed using β-actin antibody (Cell signaling, USA; dilution 1:200, 3% skim milk in TPBS). Following the incubation with appropriate secondary antibodies conjugated with HRP (anti-mouse or anti-rabbit IgG-HRP, Thermo

Fisher Scientific, USA), immuno-reactive bands were visualized using enhanced chemiluminescence (Supersignal Femto and Pico reagents for the detection of cABCB1 and β-actin, respectively; Thermo Fisher Scientific, USA) and ImageQuant LAS4000 instrument (GE healthcare, NJ, USA).

Generation of shRNA-transfected MDCKII cell lines

To biochemically suppress the expression of endogenous cABCB1, plasmid constructs containing shRNA against cABCB1 (cABCB1-shRNA; GenePharma, Shanghai, China) were custom designed and introduced to both MDCKII/WT and MDCKII/hABCG2 cells. The transfection of cABCB1-shRNA was carried out with FuGENE® HD Transfection Reagent (Promega, Madison, WI) according to the manufacturer's instructions. Briefly, parental MDCKII cells were seeded in a 12-well plate 24 hours prior to the transfection. Two μg of cABCB1-shRNA was added to a mixture consisting of 6 μL of the transfection reagent and 100 μL Opti-MEM (Rockville, Maryland, USA): The solution was added to MDCKII cells for transfection. The cells were then transferred to a 100-mm dish after 24 hours of the transfection. Hygromycin, the selection agent, was introduced on the next day at a concentration of 0.2 mg/mL. The selection media were maintained for at least 14 days to select the clone(s) resistant to the antibiotics. The clones were further screened for their functional activity of cABCB1 by comparing the P_{app} and ER of [^{3}H]-digoxin (primarily a substrate for cABCB1; along with unlabeled digoxin; the final total concentration of digoxin to be 1 μM) with bi-directional transport assays (Table 2). In addition, a qPCR study was carried out to confirm that the expression level of *cABCB1* was reduced in the shRNA-transfected clones, compared to that in non-transfected MDCKII/WT. In the clones showing a marked decrease in digoxin efflux (i.e., from ER of approximately 7 to less than 1.3), the cABCB1 mRNA levels were also reduced by > 70% compared to non-transfected cells (the

cABCB1 protein levels also decreased, Fig. S3, Supplemental material). Therefore, these clones were considered to have biochemically suppressed cABCB1 expression and were used in subsequent studies.

Evaluation of representative human ABCB1 inhibitors for their inhibitory potency toward cABCB1 in MDCKII cells

For the evaluation of the inhibitory potency of representative ABCB1 inhibitors [i.e., tariquidar, cyclosporine A, zosuquidar, and verapamil (Stephens et al., 2001; Taub et al., 2005; Agarwal et al., 2010; Römermann et al., 2015)] toward cABCB1, the basolateral to apical or apical to basolateral transport of [^{3}H]-digoxin (primarily a substrate for cABCB1; along with unlabeled digoxin; with the final total concentration of digoxin being 1 μM) was determined in MDCKII/WT in the presence of various concentrations of inhibitors. In addition, the transport of [^{3}H]-prazosin (primarily a substrate for hABCG2; along with unlabeled prazosin, the final total concentration of prazosin being 1 μM) was examined in MDCKII/hABCG2 for the evaluation of the inhibitory potency of the inhibitors toward hABCG2.

Bi-directional transport studies were carried out as described previously (Jeong et al., 2017). Briefly, MDCKII cells were seeded on Transwell® filters (12 mm diameter, 0.4 μm pore size; Corning, USA) at a density of 0.5×10^6 cells·mL^{-1}, and then cultured for 5-6 days before being used in transport assays. Transport was initiated by adding transport buffer containing the substrate (i.e., digoxin or prazosin) to the donor compartment, followed by incubation at 37°C for 120 min. Aliquots (300 μL) of the receiver and donor samples were collected at the end of the incubation. Scintillation fluid (Ultima Gold, Perkin Elmer, USA) was subsequently added to the samples and the radioactivity determined by liquid scintillation counting (Tri-Carb 3110 TR, Perkin Elmer, USA). In this study, the final

concentration of DMSO (i.e., an agent used for the solubilization of ABCB1 inhibitors) in the transport buffer was equal to or below 0.1% in all inhibition experiments except for cyclosporine A (i.e., final concentration of DMSO was 0.5%). From our preliminary experiment, DMSO at a concentration below 1% in the transport medium was found to have no appreciable impact on transporter function, consistent with other literature findings (Taub et al., 2002).

Transcellular transport of dual substrates of ABCB1 and ABCG2

The transcellular transport of dual substrates of ABCB1 and ABCG2 (e.g., irinotecan and topotecan; final concentration of 10 μM) was determined in the presence of 100 μM verapamil in MDCKII/WT and MDCKII/hABCG2 cells (i.e., subsequently referred to as 'verapamil-treated') or in MDCKII/WT and MDCKII/hABCG2 cells expressing cABCB1-shRNA (i.e., subsequently referred to as 'shRNA-transfected'). Olaparib was also included (i.e., at a final concentration of 10 μM) in this transport assay, since the drug could potentially serve as a substrate for both transporters. The transport of the dual substrates was studied for a period of 120 min at 37˚C. When necessary, 1 μM Ko143 (i.e., a standard inhibitor of hABCG2; Figure S5, Supplemental materials) was added to the transport media to further confirm hABCG2-mediated transport. For the chromatographic quantification of the dual substrates, previously reported assays were used with minor modifications (Luo et al., 2002; Vries et al., 2007; Sparidans et al., 2011). In this study, the system was equipped with a Waters e2695 high-performance liquid chromatography system (Milford, MA) and an API 3200 QTRAP mass spectrometer (Applied Biosystems, Foster City, CA). Separations were carried out using a linear gradient of 0.1% formic acid in methanol and 0.1% formic acid in water at a flow rate of 0.25 mL/min with a reversed-phase high-performance LC column (Agilent Eclipse XDB-C18, 3.5 mm, 2.1 × 100 mm). Samples were monitored at the

following Q1/Q3 transitions (m/z): 587.2/124.1 for irinotecan, 422.9/378.0 for topotecan, 435.2/281.0 for olaparib and 281.3/86.1 for imipramine (i.e., an internal standard of the assay). The specificity, linearity, precision and accuracy of the assay were found to be within the acceptance criteria of the guidelines of assay validation (FDA, 2013). The limit of quantification was 10, 20 and 10 nM for irinotecan, topotecan and olaparib, respectively.

Transcellular transport of olaparib in LLC-PK1 cells

The transcellular transport of olaparib was also determined in hABCG2-overexpressing LLC-PK1 cells. Cells were seeded onto Transwell ® filters (12 mm diameter, 0.4 μm pore size; Corning, USA) at a density of 0.5×10^6 cells·mL^{-1}, and cultured for 5-6 days prior to the transport assays. Transport was initiated by adding transport buffer containing 10 μM olaparib to the donor compartment, followed by incubation at 37°C for 120 min. When necessary, 1 μM Ko143 (i.e., a standard inhibitor of hABCG2) was included in the transport media. Aliquots of the donor and receiver samples were collected at the end of the incubation, and were subjected to chromatographic quantification as described above.

Data analysis

When it was necessary to estimate the apparent permeability coefficient (P_{app}), the following equation was used (Eq. 1):

$$P_{app} = \frac{1}{A} \times \frac{1}{C_0} \times \frac{dQ}{dt} \qquad (1)$$

where *dQ/dt*, *A* and C_0 represent the transport rate, the surface area of the insert and the initial concentration of the compound in the donor compartment, respectively. ER was calculated by dividing the basolateral to apical P_{app} by the apical to basolateral P_{app} (Wang et

al., 2005). In inhibition studies, the % ER was also calculated by dividing the value for ER in the presence of the inhibitor by that without the inhibitor (i.e., control). When necessary, the % ER value was used to evaluate the half maximal inhibitory concentration (IC_{50}) by a nonlinear regression analysis using Winnonlin Professional 5.0.1 software (Pharsight Corporation, Mountain View, CA) and the following equation (Eq. 2):

$$V = V_{max} - (V_{max} - V_0) \times \left[\frac{[I]}{[I] + IC_{50}}\right] \qquad (2)$$

where V, V_{max}, V_0 and [I] are the rate of transport in the presence of inhibitor, the maximal rate of transport, the basal rate of transport, and the concentration of inhibitor, respectively. Assuming the mechanism of inhibition to be competitive, the inhibitory constant (K_i) of the inhibitor was calculated for the estimated IC_{50} by using the following equation (Eq. 3) (Cheng and Prusoff, 1973) :

$$K_i = \frac{IC_{50}}{1 + \frac{[S]}{K_m}} \qquad (3)$$

where [S] is concentration of the substrate and K_m represents the Michaelis-Menten constant. For the comparison of apparent selectivity of cABCB1 inhibitors, the ratio of K_i values [i.e., dividing $K_{i,hABCG2}$ (i.e., estimated K_i with MDCKII/hABCG2) to $K_{i,cABCB1}$ (i.e., estimated K_i with MDCKII/WT)] was calculated for the inhibitors.

When it was necessary, 'corrected' efflux ratio (cER) was calculated by dividing the ER obtained in MDCKII/hABCG2 by the ER obtained in MDCKII/WT (Eq. 4):

$$cER = \frac{ER_{MDCKII/hABCG2}}{ER_{MDCKII/WT}} \qquad (4)$$

Statistics

For the comparison of means between / amongst groups, the two-tailed/unpaired Student's *t*-test (for qPCR studies), or the one-way ANOVA (analysis of variance; for bi-directional transport studies), followed by Tukey's *post hoc* test, was used. In this study, a value of $P < 0.05$ was considered to denote statistical significance.

Results

Variable expression of cABCB1 in MDCKII cell lines

We compared the endogenous expression of cABCB1 between MDCKII/WT and MDCKII/hABCG2 cells. The qPCR results indicated that the levels of *cABCB1* mRNA was by approximately 60% lower in MDCKII/hABCG2 than in MDCKII/WT (Fig. 1A, n=3 independently prepared sets). The mRNA levels of canine *ABCG2* were quite low with the threshold cycles greater than 33 in both MDCKII/WT and MDCKII/hABCG2, consistent with a literature report indicating that canine *ABCG2* is not abundantly expressed in MDCKII cells (data not shown) (Di et al., 2011). The observed downregulation of *cABCB1* mRNA was accompanied by a decrease in the cABCB1 protein level. When the immunoblotting analysis was performed using the commonly used ABCB1 antibody C219 [which can react with cABCB1 (Ito et al., 1999; Kuteykin-Teplyakov et al., 2010; Römermann et al., 2015)], multiple immunoreactive bands were detected. The band near 130 kDa likely comes from cross-reactivity with ABCB4 according to the previous reports (Schinkel et al., 1991; Scheffer et al., 2000). Thus, the densitometric analysis was performed on the two upper bands with their electrophoretic mobility of 150 - 170 kDa, likely arising from differing degrees of post-translational modifications including glycosylation, as reported previously (Tang et al., 2002). When the band intensities were compared using 3 independently prepared sets of samples, MDCKII/hABCG2 cells displayed the cABCB1 protein levels lower than MDCKII/WT cells (on average by 55%, Fig. 1B). Among the independently prepared samples (passage number differences within 5), the levels of cABCB1 protein also varied. Intriguingly, the cABCB1 level was consistently lower in the MDCKII/hABCG2 cells than MDCKII/WT cells. These collective observations indicate that the expression of cABCB1 in MDCKII cells was reduced in MDCKII/hABCG2, compared with MDCKII/WT. We

reasoned that the downregulation of cABCB1 may lead to a violation of the assumption regarding the consistency of baseline transport, thereby negatively impacting the accuracy of cER, especially for dual substrates of cABCB1 and hABCG2.

Differential inhibition of cABCB1 and hABCG2 in MDCKII/hABCG2 cells in the presence of human ABCB1 inhibitors

In this study, the comparative selectivity of commercially available human ABCB1 inhibitors [i.e., tariquidar, cyclosporine A, zosuquidar and verapamil (Stephens et al., 2001; Taub et al., 2005; Agarwal et al., 2010; Römermann et al., 2015)] towards cABCB1 and hABCG2 was examined in MDCKII/WT and MDCKII/hABCG2 cells. The apical to basolateral and basolateral to apical transport of digoxin (i.e., an index for cABCB1 function) were measured in the presence of various levels of inhibitors and IC_{50} / K_i values calculated (Table 1 and Fig. 2). Tariquidar was found to be an inadequate inhibitor of cABCB1 at the concentration (i.e., 0.2 μM) reported for inhibiting ABCB1 (Römermann et al., 2015). Furthermore, at higher concentrations, tariquidar and cyclosporine A were both found to be significant inhibitor of both cABCB1 and hABCG2: K_i values toward hABCG2 and cABCB1 were not substantially different between each other (i.e., fold differences of less than 10). hABCG2 was not inhibited by any of the concentrations of zosuquidar tested. However, this inhibitor had limited solubility in the aqueous media of the transport study and it was not possible to increase its concentration further. Therefore, based on the kinetic estimates of K_i, the difference in the K_i values for the transporters was calculated to be approximately 16.2 for zosuquidar. Amongst the inhibitors studied, verapamil showed a relatively higher selectivity for the inhibition toward cABCB1 (i.e., K_i ratio of 191, indicating a 191-fold lower K_i value towards cABCB1). In subsequent studies, the presence of verapamil at a concentration of 100 μM (Fig. 3 and 4) was assumed to have functional inhibition toward

cABCB1 with no appreciable inhibition toward hABCG2. In addition, our sensitivity analysis indicated that verapamil at 100 μM would permit an adequate selectivity to be maintained in a wide range of substrates having K_m values from 1 to 100 μM (Fig. S4, Supplemental material).

Transport of dual substrates in the presence of the functional inhibition / reduced expression of cABCB1 in MDCKII cells

To determine whether suppressing the function and expression of cABCB1 would result in an improved estimation of cER, control studies were carried out using MDCKII cells in the presence of 100 μM verapamil (i.e. 'verapamil-treated') and in MDCKII cells expressing shRNA directed to cABCB1 (i.e., 'shRNA-transfected') for the dual substrates of ABCB1 and ABCG2. In this study, the ER values of digoxin (primarily a substrate for cABCB1) were reduced to close to unity in MDCKII cells under the two suppressive conditions (i.e., theoretically, an adequate suppression of cABCB1 activity/expression would result in an ER of 1) (Fig. 3A, Table 2). In contrast, the cER of prazosin (primarily a substrate for hABCG2) in the two conditions under which cABCB1 functions were suppressed appeared to be unaltered [i.e., the value remained in the range of 9.9-12.5 (Fig. 3B, Table 2; as a reference, the value for cER without suppression to be 9.6)], indicative of no meaningful reduction in hABCG2 function under conditions where cABCB1 function was suppressed. As expected, the ER values were high for olaparib, irinotecan and topotecan (i.e., dual substrates) in MDCKII/WT without suppression, while the values were reduced to close to unity when cABCB1 function was inhibited, either kinetically or biochemically (Fig. 3A, Table 2) in MDCKII/WT cells. As a result, the cER values of irinotecan and topotecan were elevated by 4.8-fold and 2.3-fold in the case of the verapamil treatment, and 4.5-fold and 2.4-fold in the shRNA-transfected case (Fig. 3B, Table 2). Collectively, the above observations suggest that

the two suppressive methods are both effective in improving the cER estimation for dual substrates of ABCB1/ABCG2 in MDCKII cells expressing hABCG2.

Estimation of the cER for olaparib in MDCKII cells expressing hABCG2 under the functional suppression of cABCB1

In this study, we found that the ER values for olaparib in MDCKII/hABCG2 and MDCKII/WT were comparable (Fig. 4A; viz, cER estimation close to 1), suggesting that olaparib is not a substrate for hABCG2, consistent with previously published observations (McCormick and Swaisland, 2016). In contrast, however, in the presence of Ko143, the ER for olaparib in MDCKII/hABCG2 was significantly decreased (Fig. 4A). Under verapamil-treatment conditions, the ER in MDCKII/WT was markedly reduced but the extent of the reduction was less in MDCKII/hABCG2. Similarly, the ER for olaparib was markedly decreased in shRNA-transfected MDCKII/WT. As a result, the cER of olaparib was 2.81 ± 0.376 (verapamil-treatment conditions, $P < 0.01$) or 4.62 ± 0.421 (shRNA-transfected condition, $P < 0.01$), compared to 0.926 ± 0.0889 (without cABCB1 suppression). The addition of Ko143 resulted in a further reduction in the ER ($P < 0.01$; Fig. 4B and 4C). Furthermore, addition of elacridar and fumitremorgin C also resulted in reduction of the ER to 0.97-1.20 (Fig. S6, Supplemental material). Collectively, these observations indicate that the possibility of hABCG2-mediated transport cannot be excluded for olaparib.

Human ABCG2-mediated transport of olaparib in hABCG2-overexpressing LLC-PK1

When transcellular transport of olaparib was determined in hABCG2-overexpressing LLC-PK1 (LLC-PK1/hABCG2), ER was significantly elevated for olaparib compared to LLC-PK1/WT or LLC-PK1/Mock cells, resulting in cER of 1.88 ± 0.192 or 2.20 ± 0.571,

respectively. Upon addition of Ko143, the ER value was reduced comparable to control cells (Fig. 5).

Discussion

The findings reported in this study indicate that cABCB1 expression was statistically reduced in MDCKII cells expressing hABCG2 (Fig. 1) in comparison to that in wild type MDCKII cells. As previously noted in the literature, the expression of endogenous transporters can be downregulated as a compensatory response to the transfection and elevated expression of exogenous transporters sharing substrates (Lloyd et al., 1992; Litman et al., 2001; Agarwal et al., 2011). In addition, routine batch-to-batch or passage-dependent differences may manifest alteration(s) in the expression of endogenous transporters (Kuteykin-Teplyakov et al., 2010; Di et al., 2011; Gartzke and Fricker, 2014). Our current study was aimed to examine the robustness of cER in relation to hABCG2, and to study experimental methodologies (i.e., kinetic/biochemical suppression) for improving the cER estimation accuracy under fluctuating levels of endogenous cABCB1. Thus, the molecular mechanisms underlying the observed down-regulation of cABCB1 or any causal relationship between the changes in hABCG2 and cABCB1 was not directly examined. To our knowledge, our observation represents the first to document that estimating cER can become unreliable for dual substrates of ABCB1 and ABCG2 by the variable expression of cABCB1 in MDCKII cells. In the literature, it was previously noted that the functional expression of cABCB1 was reduced in MDCKII cells after the expression of human ABCB1 (Kuteykin-Teplyakov et al., 2010; Li et al., 2013). Taken together, variations in the expression of cABCB1 may not be uncommon in MDCKII cells, especially when foreign transporter gene(s) is (are) introduced into the cell line. In particular, our results, as well as others (Kuteykin-Teplyakov et al., 2010; Li et al., 2013) clearly demonstrate that the variable expression of cABCB1 was associated with an incorrect estimation of cER leading to inadequate phenotyping of the compounds toward efflux transporters. Considering a number of substrates shared between ABCB1 and ABCG2 (Litman et al., 2001; Agarwal et al., 2011),

the possibility of inadequate transporter phenotyping for dual substrates of ABCB1/ABCG2, such as olaparib, cannot be excluded under conditions where the expression of endogenous ABCB1 becomes variable. The careful use of cER in transporter phenotyping is, therefore, warranted in studies when dual substrates of ABCB1/ABCG2 are being studied in cells expressing these transporters.

In this study, the activity of cABCB1 was suppressed, kinetically or biochemically, in an attempt to minimize the contribution of the endogenous efflux system and to improve cER estimation in MDCKII cells. In our kinetic suppression approach, we first screened the selectivity of four well-known inhibitors of human ABCB1 (zosuquidar, tariquidar, verapamil and cyclosporine A) against the transport of digoxin (i.e., primarily transported by cABCB1) and prazosin (i.e., primarily transported by hABCG2). We found that verapamil was the most selective toward cABCB1 against hABCG2 (e.g., 191-fold lower K_i value towards cABCB1, Table 1). In parallel, the biochemical suppression on the expression of cABCB1 was also attempted in MDCKII cells using an shRNA approach. In these two separate experimental designs, the basal to apical transport of digoxin was significantly depressed ($P < 0.01$), in comparison to untreated MDCKII/WT (Table 2), with ER values in the range from 1.0 to 1.3 for digoxin in the case of kinetic and biochemical suppression, respectively, suggesting that these two methods are equally effective in suppressing the contribution of cABCB1. Consistent with this statement, the cER values obtained in the two methods were quite comparable for the three dual substrates (e.g., irinotecan, topotecan and olaparib) of the two efflux transporters (Fig. 3B). Other methods for suppressing cABCB1 function [e.g., the CRISPR-Cas9 dependent knock-out of cABCB1 (Simoff et al., 2016; Karlgren et al., 2017)] may also be used to improve the reliability of the estimation of cER, although the generation and validation of such an experimental system would likely be time-consuming. For the case

of the kinetic suppression approach, a selection procedure would not be necessary for this method, which would make it immediately applicable.

It was previously reported that, using an experimental system essentially identical to that used in the current study, hABCG2-mediated efflux was not likely for olaparib, since the cER value was calculated to be 0.5-1.0 in the study (CHMP, 2014; McCormick and Swaisland, 2016). In the literature, it was also found that Sf9 membrane vesicle ATPase study was incapable of identifying olaparib as a substrate of hABCG2 (CHMP, 2014). However, it is noteworthy that the principle of the ATPase assay is the estimation of the activity of the transporter through the detection of ATP hydrolysis rather than a direct measurement of the transported substrate itself. Such indirect activity assessment may be more prone to errors, particular for substrates transported at a reduced rate, viz weak substrates (Glavinas et al., 2008; Zhang and Surapaneni, 2012; Polli et al., 2001). Interestingly, a distinct decrease was previously noted for basolateral to apical P_{app} in the presence of Ko143 (i.e., a standard inhibitor for ABCG2) (McCormick and Swaisland, 2016), thus contradicting the conclusion for the cER estimation described in an assessment report from the European Medicines Agency (CHMP, 2014). In our study, the cER of olaparib was found to be 2.81 ± 0.376 (kinetic suppression approach, $P < 0.01$) or 4.62 ± 0.421 (biochemical suppression approach, $P < 0.01$), compared to 0.926 ± 0.0889 (without cABCB1 suppression) (Fig. 4), suggesting that hABCG2-mediated efflux cannot be ruled out for olaparib. In addition, cER was estimated to be close to 2 in hABCG2-overexpressing LLC-PK1 cells, suggesting that hABCG2-mediated transport of olaparib is not limited to one cell system.

Olaparib is an orally active, small molecule inhibitor of poly ADP-ribose polymerase (PARP): This PARP inhibitor was recently approved for the treatment of advanced ovarian cancer and BRCA-mutated metastatic breast cancer with the possibility of applications to other cancer types as well (Robert et al., 2017). Since olaparib was previously regarded

primarily as a substrate for ABCB1, the decrease in intracellular exposure in cancer cells was thought to be entirely mediated by ABCB1 (Vaidyanathan et al., 2016). However, considering the possibility of ABCG2-mediated transport for olaparib, collaborative efflux transport via ABCB1 and ABCG2 may be a distinct possibility for the PARP inhibitor in cells/tissues expressing the two transporters. Increased expression of ABCG2 was observed in tumor bearing mice (Rottenberg et al., 2008) or a triple negative breast cancer cell line (Dufour et al., 2015) that had been exposed to olaparib, although the increase was significantly less than that observed for ABCB1. Therefore, further studies are warranted for a complete understanding of the involvement of ABCG2 in the *in vivo* pharmacokinetics and pharmacodynamics of olaparib.

In conclusion, the expression of cABCB1 was found to be variable in MDCKII cells expressing hABCG2 in comparison with untreated MDCKII cells. Both kinetic (i.e., the presence of 100 μM verapamil) or biochemical (i.e., the expression of cABCB1-targeting shRNA) suppression of cABCB1 appeared to be effective in reducing the contribution of cABCB1, leading to an improved estimation of cER for dual substrates of ABCB1 and ABCG2 in MDCKII cells. It is particularly noteworthy that the cER for olaparib under conditions where the function of cABCB1 is suppressed was consistently greater than 2 in MDCKII/hABCG2 cells, suggesting that hABCG2-mediated efflux cannot be ruled out for olaparib.

Authorship Contributions

Participated in research design: Song and Chung.

Conducted experiments: Song, Park, Oh, Hyung, Kim and Jeong.

Performed data analysis: Song, Jeong, and Chung.

Wrote or contributed to the writing of the manuscript: Song, Park, Oh, Hyung, Jeong, Kim, Lee and Chung.

References

Agarwal S, Hartz AM, Elmquist WF and Bauer B (2011) Breast cancer resistance protein and P-glycoprotein in brain cancer: two gatekeepers team up. *Curr Pharm Des* **17**:2793-2802.

Agarwal S, Sane R, Gallardo JL, Ohlfest JR and Elmquist WF (2010) Distribution of gefitinib to the brain is limited by P-glycoprotein (ABCB1) and breast cancer resistance protein (ABCG2)-mediated active efflux. *J Pharmacol Exp Ther* **334**:147-155.

Allen JD, van Loevezijn A, Lakhai JM, van der Valk M, van Tellingen O, Reid G, Schellens JH, Koomen GJ and Schinkel AH (2002) Potent and specific inhibition of the breast cancer resistance protein multidrug transporter in vitro and in mouse intestine by a novel analogue of fumitremorgin C. *Mol Cancer Ther* **1**:417-425.

Cheng Y-C and Prusoff WH (1973) Relationship between the inhibition constant (Ki) and the concentration of inhibitor which causes 50 per cent inhibition (I50) of an enzymatic reaction. *Biochem Pharmacol* **22**:3099-3108.

CHMP (2014) CHMP assessment report : Lynparza. *CHMP assessment report*.

Di L, Whitney-Pickett C, Umland JP, Zhang H, Zhang X, Gebhard DF, Lai Y, Federico JJ, Davidson RE and Smith R (2011) Development of a new permeability assay using low-efflux MDCKII cells. *J Pharm Sci* **100**:4974-4985.

Dufour R, Daumar P, Mounetou E, Aubel C, Kwiatkowski F, Abrial C, Vatoux C, Penault-Llorca F and Bamdad M (2015) BCRP and P-gp relay overexpression in triple negative basal-like breast cancer cell line: a prospective role in resistance to Olaparib. *Sci Rep* **5**:12670.

FDA (2013) FDA guidance for industry: bioanalytical method validation. *US Department of Health and Human Services, Food and Drug Administration, Center for Drug Evaluation and Research (CDER)*.

FDA (2017) In Vitro Metabolism and Transporter Mediated Drug-Drug Interaction Studies : Guidance for Industry. *US Department of Health and Human Services, Food and Drug Administration, Center for Drug Evaluation and Research (CDER)*.

Gartzke D, Delzer J, Laplanche L, Uchida Y, Hoshi Y, Tachikawa M, Terasaki T, Sydor J and Fricker G (2015) Genomic Knockout of Endogenous Canine P-Glycoprotein in Wild-Type, Human P-Glycoprotein and Human BCRP Transfected MDCKII Cell Lines by Zinc Finger Nucleases. *Pharm Res* **32**:2060-2071.

Gartzke D and Fricker G (2014) Establishment of optimized MDCK cell lines for reliable efflux transport studies. *J Pharm Sci* **103**:1298-1304.

Goh L-B, Spears KJ, Yao D, Ayrton A, Morgan P, Wolf CR and Friedberg T (2002) Endogenous drug transporters in in vitro and in vivo models for the prediction of drug disposition in man. *Biochem Pharmacol* **64**:1569-1578.

Hyung S, Pyeon W, Park JE, Song YK and Chung SJ (2017) The conditional stimulation of rat organic cation transporter 2, but not its human ortholog, by mesoridazine: the possibility of the involvement of the high-affinity binding site of the transporter in the stimulation. *J Pharm Pharmacol* **69**:1513-1523.

Ito S, Woodland C, Sarkadi B, Hockmann G, Walker SE and Koren G (1999) Modeling of P-glycoprotein-involved epithelial drug transport in MDCK cells. *Am J Physiol Renal Physiol* **277**:F84-F96.

Jeong Y-S, Yim C-S, Ryu H-M, Noh C-K, Song Y-K and Chung S-J (2017) Estimation of the minimum permeability coefficient in rats for perfusion-limited tissue distribution

in whole-body physiologically-based pharmacokinetics. *Eur J Pharm Biopharm* **115**:1-17.

Karlgren M, Simoff I, Backlund M, Wegler C, Keiser M, Handin N, Muller J, Lundquist P, Jareborg AC, Oswald S and Artursson P (2017) A CRISPR-Cas9 Generated MDCK Cell Line Expressing Human MDR1 Without Endogenous Canine MDR1 (cABCB1): An Improved Tool for Drug Efflux Studies. *J Pharm Sci* **106**:2909-2913.

Kuteykin-Teplyakov K, Luna-Tortos C, Ambroziak K and Loscher W (2010) Differences in the expression of endogenous efflux transporters in MDR1-transfected versus wildtype cell lines affect P-glycoprotein mediated drug transport. *Br J Pharmacol* **160**:1453-1463.

Laemmli UK (1970) Cleavage of structural proteins during the assembly of the head of bacteriophage T4. *nature* **227**:680-685.

Lee JH, Noh CK, Yim CS, Jeong YS, Ahn SH, Lee W, Kim DD and Chung SJ (2015) Kinetics of the Absorption, Distribution, Metabolism, and Excretion of Lobeglitazone, a Novel Activator of Peroxisome Proliferator-Activated Receptor Gamma in Rats. *J Pharm Sci* **104**:3049-3059.

Lepist E-I, Phan TK, Roy A, Tong L, MacLennan K, Murray B and Ray AS (2012) Cobicistat boosts the intestinal absorption of transport substrates, including HIV protease inhibitors and GS-7340, in vitro. *Antimicrob Agents Chemother* **56**:5409-5413.

Li J, Wang Y and Hidalgo IJ (2013) Kinetic analysis of human and canine P-glycoprotein-mediated drug transport in MDR1-MDCK cell model: approaches to reduce false-negative substrate classification. *J Pharm Sci* **102**:3436-3446.

Litman T, Druley TE, Stein WD and Bates SE (2001) From MDR to MXR: new understanding of multidrug resistance systems, their properties and clinical significance. *Cell Mol Life Sci* **58**:931-959.

Lloyd C, Schevzov G and Gunning P (1992) Transfection of nonmuscle beta-and gamma-actin genes into myoblasts elicits different feedback regulatory responses from endogenous actin genes. *J Cell Biol* **117**:787-797.

Luo FR, Paranjpe PV, Guo A, Rubin E and Sinko P (2002) Intestinal transport of irinotecan in Caco-2 cells and MDCK II cells overexpressing efflux transporters Pgp, cMOAT, and MRP1. *Drug Metab Dispos* **30**:763-770.

McCormick A and Swaisland H (2016) In vitro assessment of the roles of drug transporters in the disposition and drug-drug interaction potential of olaparib. *Xenobiotica*:1-47.

Robert M, Frenel J-S, Gourmelon C, Patsouris A, Augereau P and Campone M (2017) Olaparib for the treatment of breast cancer. *Expert Opin Investig Drugs*.

Römermann K, Helmer R and Loescher W (2015) The antiepileptic drug lamotrigine is a substrate of mouse and human breast cancer resistance protein (ABCG2). *Neuropharmacology* **93**:7-14.

Rottenberg S, Jaspers JE, Kersbergen A, van der Burg E, Nygren AO, Zander SA, Derksen PW, de Bruin M, Zevenhoven J, Lau A, Boulter R, Cranston A, O'Connor MJ, Martin NM, Borst P and Jonkers J (2008) High sensitivity of BRCA1-deficient mammary tumors to the PARP inhibitor AZD2281 alone and in combination with platinum drugs. *Proc Natl Acad Sci U S A* **105**:17079-17084.

Scharenberg CW, Harkey MA and Torok-Storb B (2002) The ABCG2 transporter is an efficient Hoechst 33342 efflux pump and is preferentially expressed by immature human hematopoietic progenitors. *Blood* **99**:507-512.

Scheffer GL, Kool M, Heijn M, de Haas M, Pijnenborg AC, Wijnholds J, van Helvoort A, de Jong MC, Hooijberg JH and Mol CA (2000) Specific detection of multidrug resistance proteins MRP1, MRP2, MRP3, MRP5, and MDR3 P-glycoprotein with a panel of monoclonal antibodies. *Cancer Research* **60**:5269-5277.

Schinkel AH, Roelofs ME and Borst P (1991) Characterization of the human MDR3 P-glycoprotein and its recognition by P-glycoprotein-specific monoclonal antibodies. *Cancer Research* **51**:2628-2635.

Siissalo S, Laitinen L, Koljonen M, Vellonen K-S, Kortejärvi H, Urtti A, Hirvonen J and Kaukonen AM (2007) Effect of cell differentiation and passage number on the expression of efflux proteins in wild type and vinblastine-induced Caco-2 cell lines. *Eur J Pharm Biopharm* **67**:548-554.

Simoff I, Karlgren M, Backlund M, Lindstrom AC, Gaugaz FZ, Matsson P and Artursson P (2016) Complete Knockout of Endogenous Mdr1 (Abcb1) in MDCK Cells by CRISPR-Cas9. *J Pharm Sci* **105**:1017-1021.

Smith PK, Krohn RI, Hermanson G, Mallia A, Gartner F, Provenzano M, Fujimoto E, Goeke N, Olson B and Klenk D (1985) Measurement of protein using bicinchoninic acid. *Analytical biochemistry* **150**:76-85.

Sparidans RW, Martens I, Valkenburg-van Iersel LB, den Hartigh J, Schellens JH and Beijnen JH (2011) Liquid chromatography–tandem mass spectrometric assay for the PARP-1 inhibitor olaparib in combination with the nitrogen mustard melphalan in human plasma. *J Chromatogr B* **879**:1851-1856.

Stephens RH, O'Neill CA, Warhurst A, Carlson GL, Rowland M and Warhurst G (2001) Kinetic profiling of P-glycoprotein-mediated drug efflux in rat and human intestinal epithelia. *J Pharmacol Exp Ther* **296**:584-591.

Tang F, Horie K and Borchardt RT (2002) Are MDCK cells transfected with the human MDR1 gene a good model of the human intestinal mucosa? *Pharm Res* **19**:765-772.

Taub ME, Kristensen L and Frokjaer S (2002) Optimized conditions for MDCK permeability and turbidimetric solubility studies using compounds representative of BCS classes I–IV. *Eur J Pharm Sci* **15**:331-340.

Taub ME, Podila L, Ely D and Almeida I (2005) Functional assessment of multiple P-glycoprotein (P-gp) probe substrates: influence of cell line and modulator concentration on P-gp activity. *Drug Metab Dispos* **33**:1679-1687.

Vaidyanathan A, Sawers L, Gannon A-L, Chakravarty P, Scott AL, Bray SE, Ferguson MJ and Smith G (2016) ABCB1 (MDR1) induction defines a common resistance mechanism in paclitaxel-and olaparib-resistant ovarian cancer cells. *Br J Cancer* **115**:431.

Vries NAd, Ouwehand M, Buckle T, Beijnen JH and van Tellingen O (2007) Determination of topotecan in human and mouse plasma and in mouse tissue homogenates by reversed-phase high-performance liquid chromatography. *Biomed Chromatogr* **21**:1191-1200.

Wang Q, Rager JD, Weinstein K, Kardos PS, Dobson GL, Li J and Hidalgo IJ (2005) Evaluation of the MDR-MDCK cell line as a permeability screen for the blood–brain barrier. *Int J Pharm* **288**:349-359.

Xia CQ, Liu N, Yang D, Miwa G and Gan LS (2005) Expression, localization, and functional characteristics of breast cancer resistance protein in Caco-2 cells. *Drug Metab Dispos* **33**:637-643.

Yim CS, Jeong YS, Lee SY, Pyeon W, Ryu HM, Lee JH, Lee KR, Maeng HJ and Chung SJ (2017) Specific Inhibition of the Distribution of Lobeglitazone to the Liver by

Atorvastatin in Rats: Evidence for a Rat Organic Anion Transporting Polypeptide 1B2-Mediated Interaction in Hepatic Transport. *Drug Metab Dispos* **45**:246-259.

Footnotes

This study was supported by a grant of the National Research Foundation of Korea (NRF) grant funded by the Korean government (MSIP) (No. 2009-0083533). In addition, a portion of this work was presented in the form of a poster at the 2017 AAPS Annual Meeting & Exposition, November 12-15, 2017, San Diego, USA.

Figure Legends

Figure 1. (A) Expression of canine ABCB1 mRNA in MDCKII/WT and MDCKII/hABCG2, as measured by qPCR (n=3). (B) Representative immunoblots for canine ABCB1 protein in MDCKII/WT and MDCKII/hABCG2 (n=3 independently prepared sets; lysates of MDCKII/hABCB1 cells were used as a positive control; β-actin was used as a gel loading control). Dagger in the ABCB1 blot indicates the non-specific band potentially arising from the interaction of the C219 antibody with ABCB4 as reported previously (Schinkel et al., 1991; Scheffer et al., 2000). Densitometric analysis was performed for the two upper bands and the relative intensities were obtained by comparing the signals of the samples within the same set. Data are expressed as the mean ± S.D.

Figure 2. Inhibitory profiles of tariquidar, cyclosporine A, zosuquidar, and verapamil against the transport of (A) digoxin in MDCKII/WT and (B) prazosin in MDCKII/hABCG2. The apparent permeability coefficient of the compounds are shown in apical to basolateral (●; a-B) and basolateral to apical (■; b-A) directions. (C) The percent of control ER (%ER) was shown together with the best-fit values generated from the nonlinear regression analysis based on Eq. 2. Asterisks indicate statistical differences (*$P < 0.05$; **$P < 0.01$; ***$P < 0.001$) from the control group (i.e., without inhibitor) by one-way ANOVA, followed by the Tukey's *post hoc* test. Data are presented as mean ± S.D. of triplicate runs.

Figure 3. (A) Estimate of ER for ABCB1 and/or ABCG2 substrate(s) in MDCKII/WT cells. (B) Estimate of cER for ABCB1 and/or ABCG2 substrate(s), calculated from ER values obtained for MDCKII/WT and MDCKII/hABCG2 cells. Key: No suppression (○), verapamil-treated (●), and shRNA-transfected (■) conditions. The dashed line in Panels A

and B indicates ER/cER at unity. Data are presented as the ER (i.e., mean P_{app} from basolateral to apical side divided by that from apical to basolateral side) or cER (i.e., ER for MDCKII/hABCG2 divided by that for MDCKII/WT), obtained from triplicate or quadruplicate runs.

Figure 4. Bi-directional transport of olaparib in the absence of any suppression (A), in the presence of verapamil treatment (B), or in the presence of shRNA-transfected (C) conditions for MDCKII/WT and MDCKII/hABCG2 cells. When necessary, Ko143, at a concentration of 1 μM (indicated as '+Ko143'), was added to the incubation mixture. ER was calculated by dividing P_{app} from basolateral to apical side to that from apical to basolateral side. Data are presented as the mean ± S.D. of three independent experiments, each with quadruplicate runs. Asterisks indicate statistical differences based on one-way ANOVA, followed by Tukey's *post hoc* test (**$P < 0.01$).

Figure 5. Bi-directional transport of olaparib in LLC-PK1/WT and LLC-PK1/hABCG2 cells. When necessary, Ko143, at a concentration of 1 μM (indicated as '+Ko143'), was added to the incubation mixture. ER was calculated by dividing P_{app} from basolateral to apical side to that from apical to basolateral side. Data are presented as the mean ± S.D. of three independent experiments, each with quadruplicate runs. Asterisks indicate statistical differences based on one-way ANOVA, followed by Tukey's *post hoc* test (*$P < 0.05$).

JPET Fast Forward. Published on November 5, 2018 as DOI: 10.1124/jpet.118.250225
This article has not been copyedited and formatted. The final version may differ from this version.

Table 1. IC_{50} and K_i values of some representative ABCB1 inhibitors

	hABCG2		cABCB1		K_i Ratio
	IC_{50} (μM)	K_i[a] (μM)	IC_{50} (μM)	K_i[a] (μM)	($K_{i,ABCG2}/K_{i,cABCB1}$)
tariquidar	2.19	2.17	0.491	0.482	4.51
cyclosporine A	4.69	4.65	0.788	0.774	6.01
zosuquidar	>10	>9.8	0.617	0.606	>16.2
verapamil	417	414	2.21	2.17	191

[a]Calculated by using K_m value of prazosin towards hABCG2 (i.e., 128 μM), and K_m value of digoxin towards cABCB1 (i.e., 53.9 μM), estimated from $P_{app,a-B}$ in MDCKII/hABCG2 and MDCKII/WT, respectively.

JPET Fast Forward. Published on November 5, 2018 as DOI: 10.1124/jpet.118.250225
This article has not been copyedited and formatted. The final version may differ from this version.

Table 2. Bi-directional transport of ABCB1 and/or ABCG2 substrate(s) for MDCKII/WT and MDCKII/hABCG2 cells.

			P_{app},a-B (10^{-6} cm/sec)	P_{app},b-A (10^{-6} cm/sec)	ER	cER
digoxin	no suppression	MDCKII/WT	1.04 ± 0.0312	6.53 ± 0.268	6.3	0.7
		MDCKII/hABCG2	1.18 ± 0.174	5.00 ± 0.734	4.2	
	verapamil-treated	MDCKII/WT	1.55 ± 0.0764	1.65 ± 0.0465	1.1	1.0
		MDCKII/hABCG2	1.81 ± 0.0974	1.99 ± 0.0893	1.1	
	shRNA-transfected	MDCKII/WT	1.32 ± 0.0286	1.72 ± 0.0932	1.3	0.8
		MDCKII/hABCG2	1.23 ± 0.290	1.26 ± 0.167	1.0	
olaparib	no suppression	MDCKII/WT	2.75 ± 0.414	27.3 ± 2.72	9.9	0.9
		MDCKII/hABCG2	2.73 ± 0.464	25.1 ± 4.56	9.2	
	verapamil-treated	MDCKII/WT	8.16 ± 0.164	13.3 ± 0.514	1.6	3.2
		MDCKII/hABCG2	4.40 ± 0.386	22.5 ± 1.99	5.1	
	shRNA-transfected	MDCKII/WT	9.35 ± 0.844	9.83 ± 0.400	1.1	4.9
		MDCKII/hABCG2	4.02 ± 0.435	20.8 ± 0.852	5.2	
irinotecan	no suppression	MDCKII/WT	0.611 ± 0.364	4.47 ± 0.573	7.3	3.0
		MDCKII/hABCG2	0.404 ± 0.147	8.95 ± 0.280	22.1	
	verapamil-treated	MDCKII/WT	1.60 ± 0.257	2.34 ± 0.150	1.5	14.3
		MDCKII/hABCG2	0.411 ± 0.150	8.62 ± 0.377	21.0	
	shRNA-transfected	MDCKII/WT	1.65 ± 0.455	1.78 ± 0.360	1.1	13.5
		MDCKII/hABCG2	0.423 ± 0.045	6.16 ± 0.263	14.6	
topotecan	no suppression	MDCKII/WT	1.06 ± 0.0521	4.10 ± 0.381	3.9	5.6
		MDCKII/hABCG2	0.452 ± 0.0880	9.84 ± 0.570	21.8	
	verapamil-treated	MDCKII/WT	1.67 ± 0.115	1.86 ± 0.134	1.1	13.1
		MDCKII/hABCG2	0.711 ± 0.140	10.3 ± 0.487	14.5	

JPET Fast Forward. Published on November 5, 2018 as DOI: 10.1124/jpet.118.250225
This article has not been copyedited and formatted. The final version may differ from this version.

	shRNA-transfected	MDCKII/WT	1.59 ± 0.155	1.06 ± 0.179	0.7	13.5
		MDCKII/hABCG2	0.618 ± 0.221	5.53 ± 0.449	9.0	
prazosin	no suppression	MDCKII/WT	16.3 ± 0.527	16.2 ± 0.683	1.0	9.6
		MDCKII/hABCG2	2.76 ± 0.110	26.1 ± 1.19	9.5	
	verapamil-treated	MDCKII/WT	17.3 ± 1.91	14.6 ± 0.880	0.8	12.5
		MDCKII/hABCG2	2.66 ± 0.126	28.0 ± 1.44	10.5	
	shRNA-transfected	MDCKII/WT	16.3 ± 0.928	15.0 ± 0.121	0.9	9.9
		MDCKII/hABCG2	3.96 ± 0.0692	35.8 ± 1.86	9.1	

JPET Fast Forward. Published on November 5, 2018 as DOI: 10.1124/jpet.118.250225
This article has not been copyedited and formatted. The final version may differ from this version.

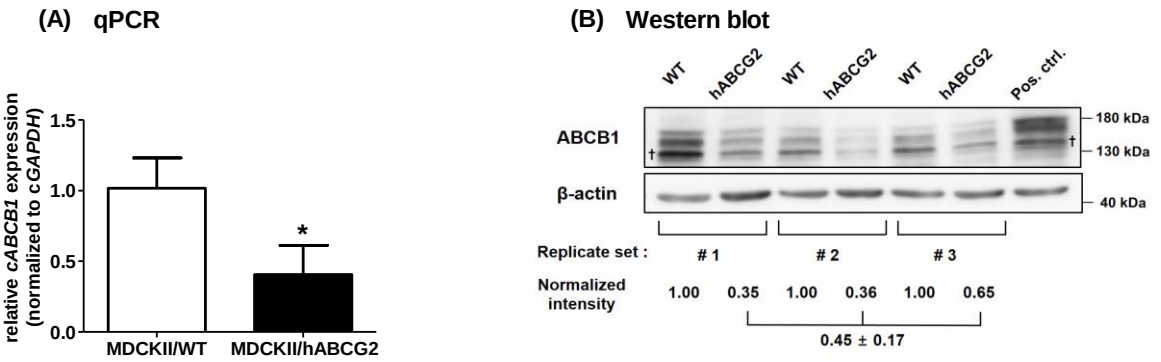

Figure 1.

JPET Fast Forward. Published on November 5, 2018 as DOI: 10.1124/jpet.118.250225
This article has not been copyedited and formatted. The final version may differ from this version.

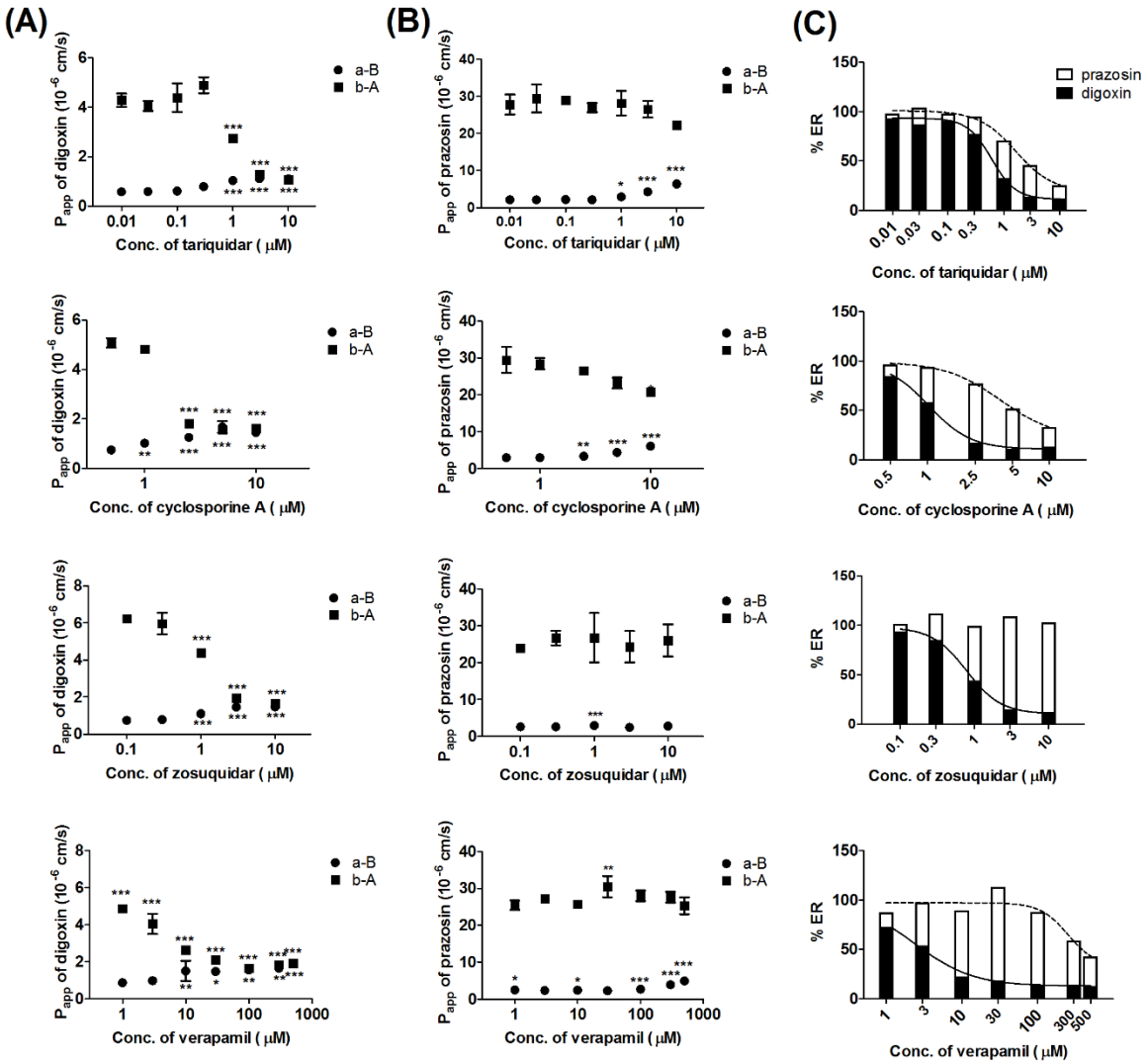

Figure 2.

JPET Fast Forward. Published on November 5, 2018 as DOI: 10.1124/jpet.118.250225
This article has not been copyedited and formatted. The final version may differ from this version.

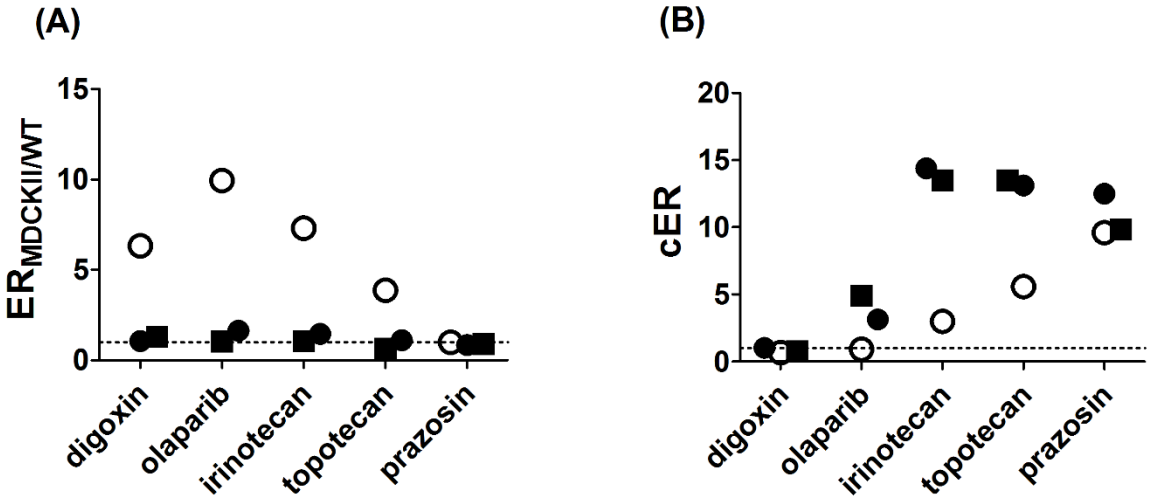

Figure 3.

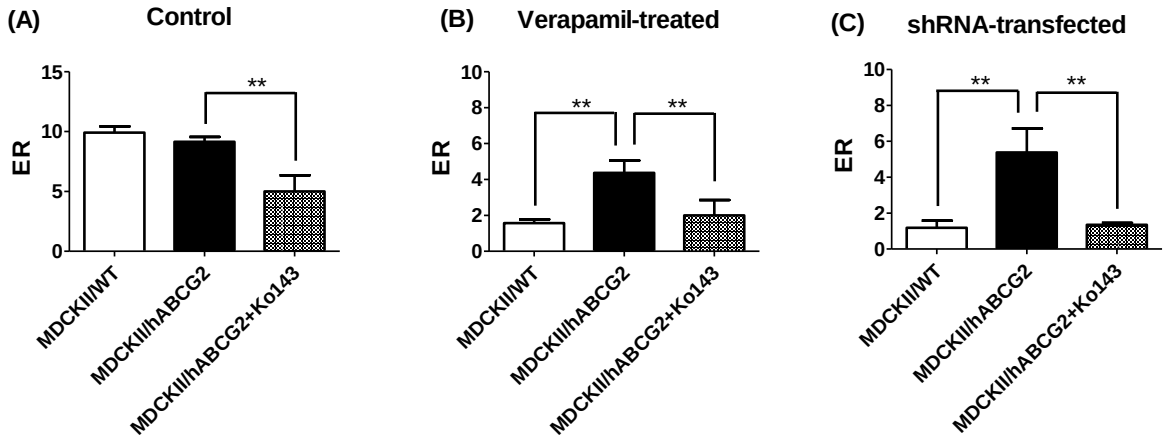

Figure 4.

JPET Fast Forward. Published on November 5, 2018 as DOI: 10.1124/jpet.118.250225
This article has not been copyedited and formatted. The final version may differ from this version.

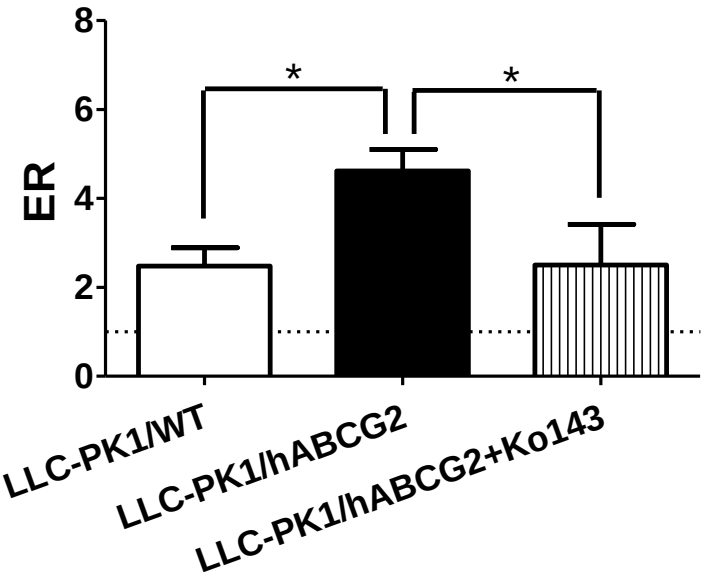

Figure 5.

Sensitivity analysis on transport inhibition of arbitrary substrates

In order to determine whether the inhibition of verapamil toward cABCB1 is applicable to an arbitrary substrate with varying K_m values, sensitivity analysis was carried out. The transport velocity of a substrate in the presence of an inhibitor is as shown in Eq. 1. In addition, IC_{50} could be described as Eq. 2 (i.e., rearrangement of Cheng-Prusoff equation), and assuming that active transport is predominant (i.e., $V_0/V_{max} = 0$), Eq. 1 could be rearranged as Eq 3 and 4:

$$V = V_{max} - (V_{max} - V_0) \cdot \left[\frac{[I]}{[I] + IC_{50}}\right] \quad (1)$$

$$IC_{50} = K_i \cdot \left(1 + \frac{[S]}{K_m}\right) \quad (2)$$

$$V = V_{max} - (V_{max} - V_0) \cdot \frac{[I]}{[I] + K_i\left(1 + \frac{[S]}{K_m}\right)} \quad (3)$$

$$\frac{V}{V_{max}} = 1 - \frac{[I]}{[I] + K_i\left(1 + \frac{[S]}{K_m}\right)} \quad (4)$$

where K_i, K_m and [S] represent the inhibition coefficient of the inhibitor, the Michaelis-Menten constant and concentration of the substrate, respectively. By using Berkeley Madonna™ software (version 8.3.18; University of California, Berkeley, CA, USA), % inhibition of the transport was then simulated using the equation below (Eq. 5):

$$\%\ inhibition = 100 \times \left(1 - \frac{V}{V_{max}}\right) \quad (5)$$

Inhibition of olaparib efflux using other ABCG2 inhibitors

To further determine hABCG2-mediated transport of olaparib, transcellular transport of olaparib was also studied in the presence of hABCG2 inhibitors other than Ko143 (i.e., elacridar or fumitremorgin C). The transcellular transport of 10 μM olaparib was determined in verapamil-treated or shRNA-transfected MDCKII/WT and MDCKII/hABCG2 cells, and 1 μM Ko143, 10 μM elacridar or 10 μM fumitremorgin C was added for inhibition of the transport. The transport was studied for a period of 120 min at 37˚C, and concentrations of olaparib were determined by chromatographic quantification at the end of the incubation.

Yoo-Kyung Song, Ji Eun Park, Yunseok Oh, Sungwoo Hyung, Yoo-Seong Jeong, Min-Soo Kim, Wooin Lee and Suk-Jae Chung : Journal of Pharmacology and Experimental Therapeutics

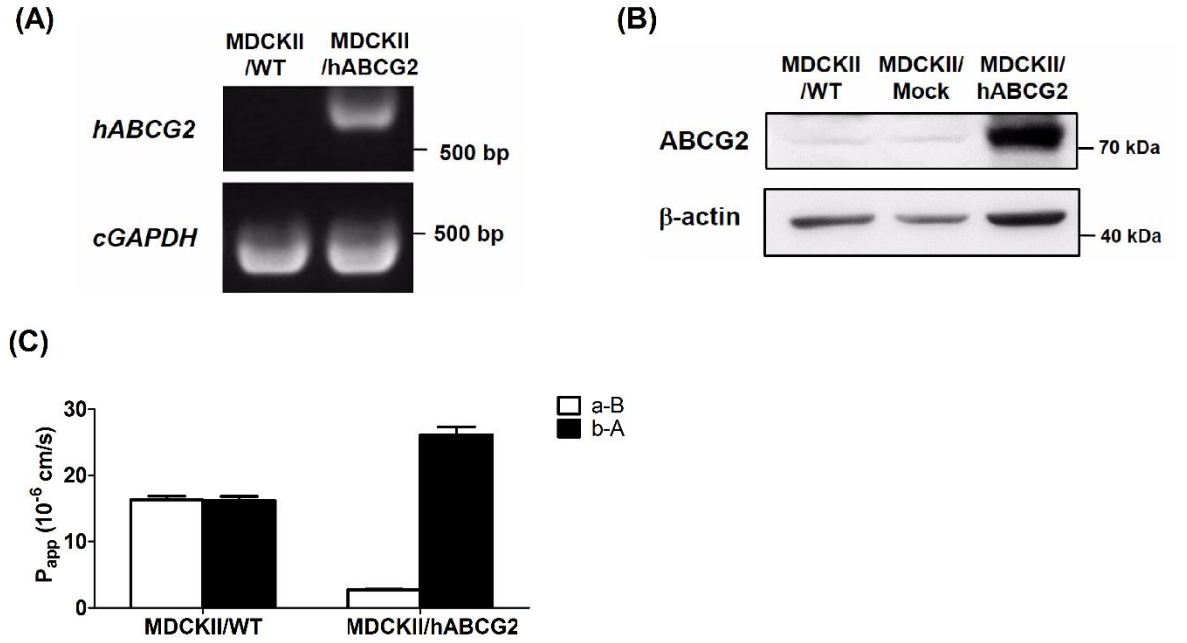

Figure S1. (A) Agarose gel electrophoresis of PCR products using the total RNA extract from MDCKII/WT and MDCKII/hABCG2 cells. PCR products were generated by *hABCG2* (product size: 577 bp) and *cGAPDH* (product size: 497 bp) primer, respectively. (B) Western blot analysis from cell lysates (60 μg) of MDCKII/WT, MDCKII/Mock and MDCKII/hABCG2, probed with anti-ABCG2 and anti-β-actin antibodies, respectively. (C) The functional expression of hABCG2 in MDCKII/hABCG2, compared to MDCKII/WT cells, as evaluated by bi-directional transport of [^{3}H]-prazosin. The apparent permeability coefficients of the compound are shown in apical to basolateral (a-B) and basolateral to apical (b-A) directions. Data are presented as mean ± S.D. of triplicate runs.

Yoo-Kyung Song, Ji Eun Park, Yunseok Oh, Sungwoo Hyung, Yoo-Seong Jeong, Min-Soo Kim, Wooin Lee and Suk-Jae Chung : Journal of Pharmacology and Experimental Therapeutics

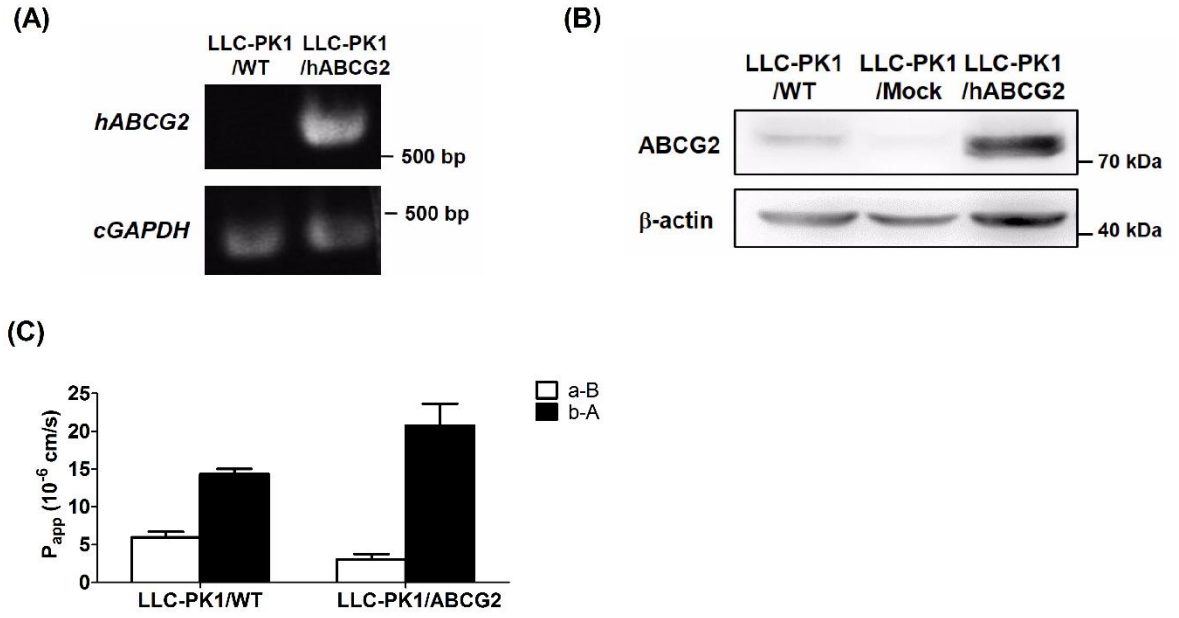

Figure S2. (A) Agarose gel electrophoresis of PCR products using the total RNA extract from LLC-PK1/WT and LLC-PK1/hABCG2 cells. PCR products were generated by *hABCG2* (product size: 577 bp) and *porcine GAPDH* (product size: 396 bp) primer, respectively. (B) Western blot analysis from cell lysates (60 μg) of LLC-PK1/WT, LLC-PK1/Mock, and LLC-PK1/hABCG2, probed with anti-ABCG2 and anti-β-actin antibodies, respectively. (C) The functional expression of hABCG2 in LLC-PK1/hABCG2, compared to LLC-PK1/WT cells, as evaluated by bi-directional transport of [^{3}H]-prazosin. The apparent permeability coefficients of the compound are shown in apical to basolateral (a-B) and basolateral to apical (b-A) directions. Data are presented as mean ± S.D. of triplicate runs.

Yoo-Kyung Song, Ji Eun Park, Yunseok Oh, Sungwoo Hyung, Yoo-Seong Jeong, Min-Soo Kim, Wooin Lee and Suk-Jae Chung : Journal of Pharmacology and Experimental Therapeutics

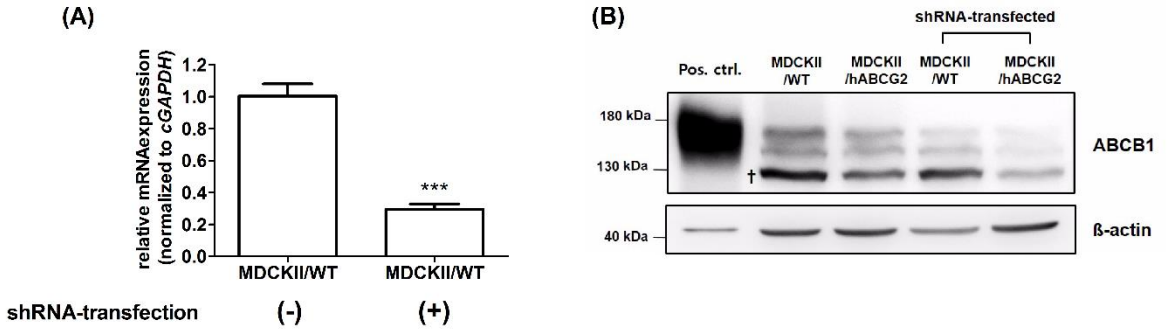

Figure S3. (A) Expression levels of *cABCB1* mRNA in shRNA-transfected and non-transfected MDCKII cell lines were evaluated by qPCR. Data are presented as mean ± S.D. of triplicate runs. Asterisks indicate statistical difference from the control (i.e., without transfection) by the unpaired t test (***$P < 0.005$). (B) Expression levels of cABCB1 protein in shRNA-transfected and non-transfected MDCKII cell lines were evaluated by Western blot. The protein amount of sample in the Western blot analysis was 200 μg for ABCB1 and 60 μg for β-actin. In parallel, 10 μg (i.e., for the detection of ABCB1) or 3 μg (i.e., for the detection of β-actin) protein was loaded for positive control (i.e., NCI/ADR-RES). Dagger in panel B indicates potential interaction of the antibody with ABCB4 (Schinkel et al., 1991; Scheffer et al., 2000).

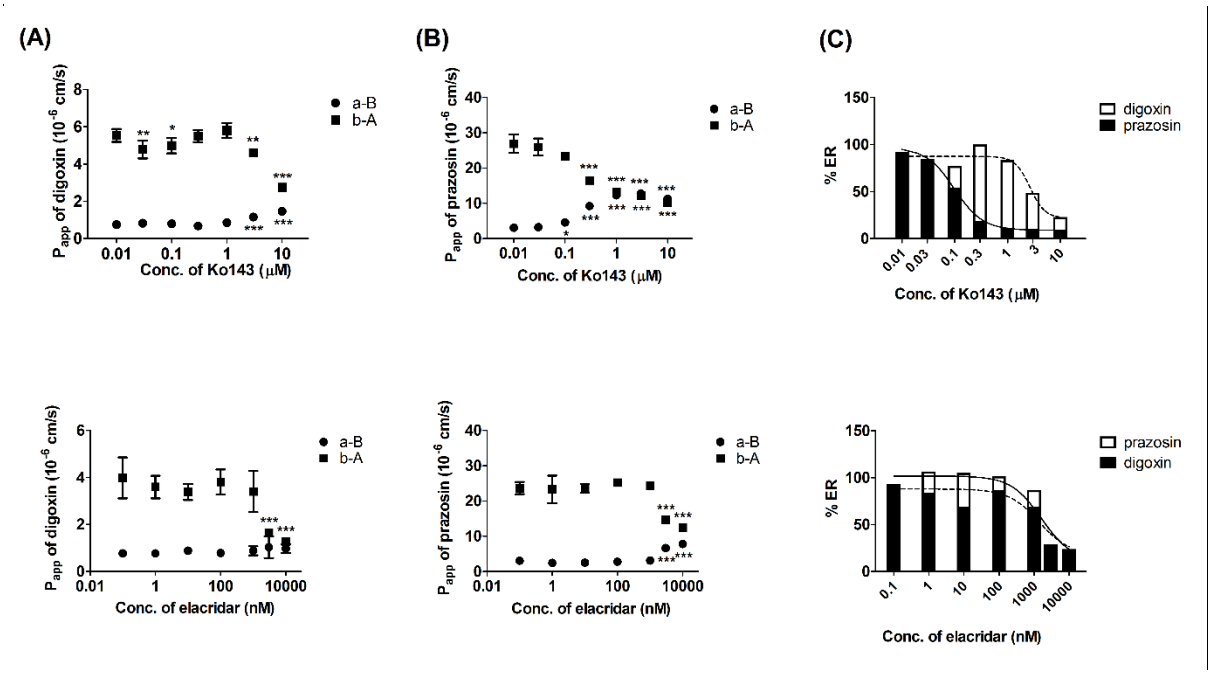

Figure S4. The inhibition profiles of Ko143 in various concentrations against the transport of digoxin in MDCKII/WT cells (A) and prazosin in MDCKII/hABCG2 cells (B) are shown in apical to basolateral (a-B) and basolateral to apical (b-A) direction. The percent of control ER (%ER) was shown together with the best-fit values obtained from the nonlinear regression analysis based on Eq. 1 (C). Similarly, the inhibition profiles of elacridar against the transport of digoxin in MDCKII/WT cells (D) and prazosin in MDCKII/hABCG2 cells (F) are shown together with the %ER values (G). Asterisks indicate statistical differences (*P < 0.05, **P < 0.01; ***P < 0.001) from the control group (i.e., without inhibitor) by one-way ANOVA, followed by the Tukey's *post hoc* test. Data are presented as mean ± S.D. of triplicate runs.

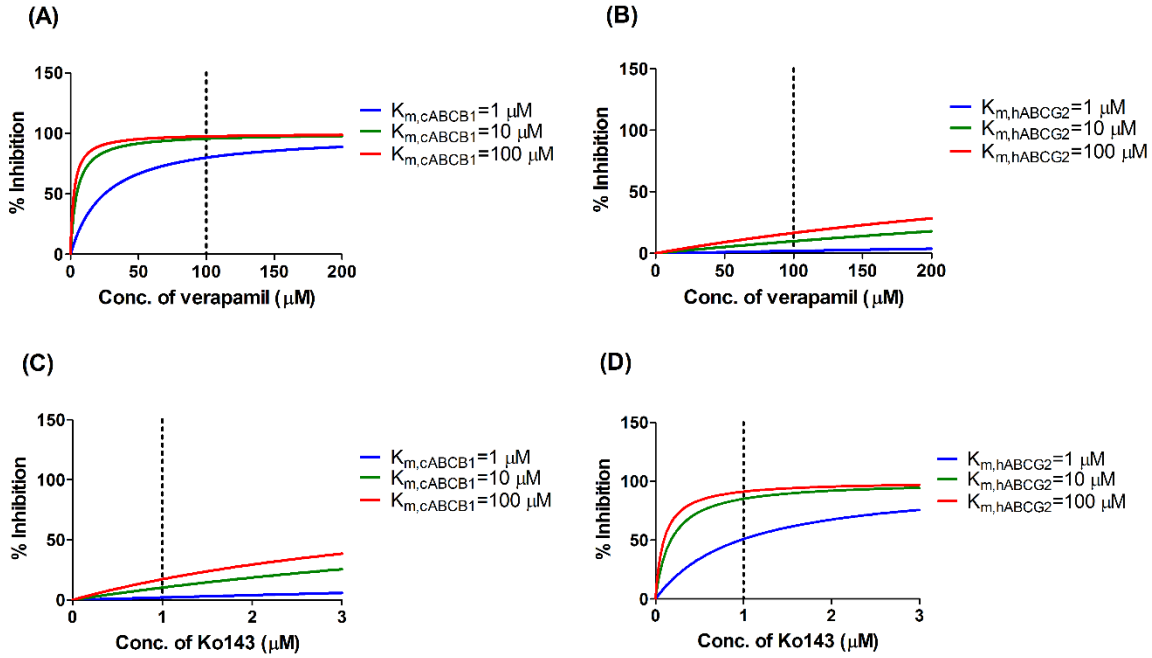

Figure S5. Sensitivity analysis of transport inhibition by 100 μM verapamil towards cABCB1 (A) and hABCG2 (B), and sensitivity analysis of transport inhibition by 1 μM Ko143 towards cABCB1 (C) and hABCG2 (D) assuming arbitrary substrate having a K_m value of 1~100 μM towards cABCB1 and hABCG2, respectively.

Yoo-Kyung Song, Ji Eun Park, Yunseok Oh, Sungwoo Hyung, Yoo-Seong Jeong, Min-Soo Kim, Wooin Lee and Suk-Jae Chung : Journal of Pharmacology and Experimental Therapeutics

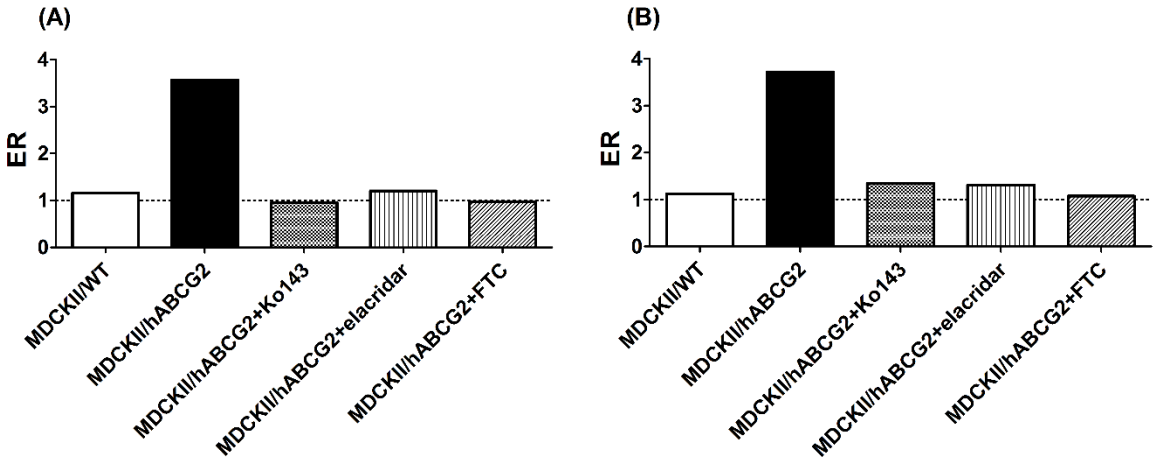

Figure S6. Bi-directional transport of olaparib in the presence of verapamil treatment (A), or in the presence of shRNA-transfected (B) conditions for MDCKII/WT and MDCKII/hABCG2 cells. When necessary, Ko143 (1 μM), elacridar (10 μM), or fumitremorgin C (FTC; 10 μM) was added to the incubation mixture.